



25th ABCM International Congress of Mechanical Engineering
October 20-25, 2019, Uberlândia, MG, Brazil

LIQUID VELOCITY PROFILES AND WALL SHEAR STRESS ESTIMATION IN WATER-AIR HORIZONTAL INTERMITTENT FLOWS

L.S. Fernandes

Pontifícia Universidade Católica do Rio de Janeiro, Department of Mechanical Engineering, 22451-900, Rio de Janeiro, RJ, Brazil
leonardofernandes@puc-rio.br

R. S. N. de Mesquita

Pontifícia Universidade Católica do Rio de Janeiro, Department of Mechanical Engineering, 22451-900, Rio de Janeiro, RJ, Brazil
rodrigonavarro@puc-rio.br

R. Y. R. de Medeiros

Pontifícia Universidade Católica do Rio de Janeiro, Department of Mechanical Engineering, 22451-900, Rio de Janeiro, RJ, Brazil
rafaelame@aluno.puc-rio.br

L.F.A. Azevedo

Pontifícia Universidade Católica do Rio de Janeiro, Department of Mechanical Engineering, 22451-900, Rio de Janeiro, RJ, Brazil
lfaa@puc-rio.br

Abstract. *The main goal of this work is to evaluate the liquid velocity profiles and estimate the wall shear stress (WSS), in the liquid plug, during intermittent gas-liquid flows in a horizontal pipe. An acrylic pipe with total length of 18m and inner diameter of 40mm was used as test section, while air and water with superficial velocities of $J_G = 0.5$ m/s and $J_L = 0.3, 0.4$ and 0.5 m/s were used as working fluid. Velocity fields measurements were performed using a high-frequency stereoscopic particle image velocimetry (SPIV) system together with the laser induced fluorescence (LIF) technique. A set of three equally-spaced photogates were used both to measure the bubble translational velocity and to trigger data acquisition, what allowed the calculation of ensemble-averaged velocity fields at equally time-spaced cross-section planes, using the gas-bubble nose tip as reference. WSS in the liquid plug was estimated based on the Clauser method, using the measured averaged velocity profiles. The small time step between each measurement plane along the slug unit cell allowed the determination of the length to the gas-bubble nose into which the velocity profile is no longer influenced by the faster moving gas bubble. The data presented are of great importance to the improvement and validation of numerical models, specially the one-dimensional ones.*

Keywords: *Intermittent flow, Wall shear stress, Gas-liquid flow, Velocity field*

1. INTRODUCTION

Two phase gas-liquid flows are present in a large number of industrial applications, ranging from nuclear power plants cooling systems to oil/gas transport and production lines. In this last example, the continuously increasing distance from satellites wells to central pre-processing facilities increases pressure and temperature variations along lines and, therefore, enhances the possibility of gas-liquid flows to happen (Hua et al., 2011). The classical gas-liquid flow maps presented in the literature (Baker, 1953; Mandhane et al., 1974; Brennen, 2005) clearly shows that there is a considerable range of liquid and gas flow rates into which the dominant flow configuration is the intermittent pattern (i.e., slug flow and elongated bubble flow).

The intermittent gas-liquid flow occurs mainly due to Kelvin-Helmoltz instability, leading to growing waves in the gas-liquid interface during a stratified flow (Taitel and Duker, 1976) or because of accumulation of liquid at lower parts of irregular terrains (Al Safran et al., 2005). Its principal characteristic is the transient flow of the phases, which can be defined by a succession of regions usually called liquid plug and gas-bubble (or liquid film). In the first region, liquid occupies the whole cross-section of the pipe, while in the last there is a gas-bubble flowing in the upper part of the pipe and liquid in the bottom. Many authors differentiate slug flow from elongated bubble flow (or plug flow) by the presence or not of dispersed gas bubbles in the liquid plug, referring to slug flow as the intermittent pattern when there are entrained bubbles in the liquid plug, originated from the gas phase ahead of it.

The transient nature of intermittent gas-liquid flow allies high mechanical loads to large variations in the flow mean density. Those characteristics can cause severe damage to both structures and equipments presented in the process (Fabre

et al. 1990). According to Kvernfold et al. (1984), the large variations in the wall shear stress can also remove anti-corrosion protections from the pipe wall, letting it vulnerable to corrosion attacks. The proper modelling of the behavior of gas-liquid intermittent flow brings, therefore, fundamental information to the proper design and operation of the pipe system.

A common practice when modelling long pipes, to avoid high computational cost is to use one-dimensional formulations. In two-phase flow, a very known model is the Two-Fluid Model (Ishii and Hibiki, 2006), which consist of a set of conservation equations for each phase. In its one dimensional formulation, the model requires the use of closure equations for shear forces and, according to Issa and Kempf (2003), its accuracy is highly dependable on the model used to calculate the wall shear stress of the liquid phase. The knowledge of the wall shear stress in the liquid phase of a gas-liquid intermittent flow can, therefore, improve and/or validate numerical simulations.

To estimate the wall shear stress in the liquid phase of an intermittent gas-liquid flow, an experiment using high-frequency Stereoscopic Particle Image Velocimetry (SPIV) together with Laser Induced Fluorescence was carried out, following the procedure described in details by Fernandes et al. (2018). The measurements allowed the calculation of ensemble-averaged velocity fields in the liquid phase of a gas-liquid intermittent flow in a horizontal pipe. The Clauser method (Wei et al., 2005) was then utilized to estimate the wall shear stress. Given the high-frequency of the system, it was also possible to determinate at which distance to the gas-bubble nose tip the velocity profiles, in the liquid plug, fully develops.

2. EXPERIMENT

The test section consisted of a horizontal 18-m long, 40-mm-diameter acrylic pipe, as shown schematically in Fig. 1. A progressive cavity pump and a radial compressor were responsible to the liquid and gas supply, respectively, which entered the pipe through a Y-mixer. A stereoscopic-PIV (SPIV) system was used to measure all three-components of the velocity vector, in cross sectional planes, in the liquid phase, of an intermittent gas-liquid flow. It consisted of a TSI 610036 Synchronizer, a Litron LDY304 laser and two high-speed Phantom M340 cameras. The system operated at a frequency of 400 Hz. The cameras were assembled around a visualization box, to minimize optical distortions. All images were processed using the software Insight 4G, from TSI. The Laser Induced Fluorescence technique was employed to separate the light scattered by the gas-liquid interfaces from that emitted by the seeding particles. Fluorescent particles with an average diameter of $10\mu\text{m}$ were used as tracers. A set of three photogates equally-spaced along the pipe length (beam-interrupter devices) were used to trigger the start of the image acquisitions by the SPIV system and to measure bubble translational velocity.

The measured bubble translational velocities (U_b) were used to convert the time between each measured velocity field into space, using the bubble nose tip as a reference. This experimental procedure was suggested in the work of

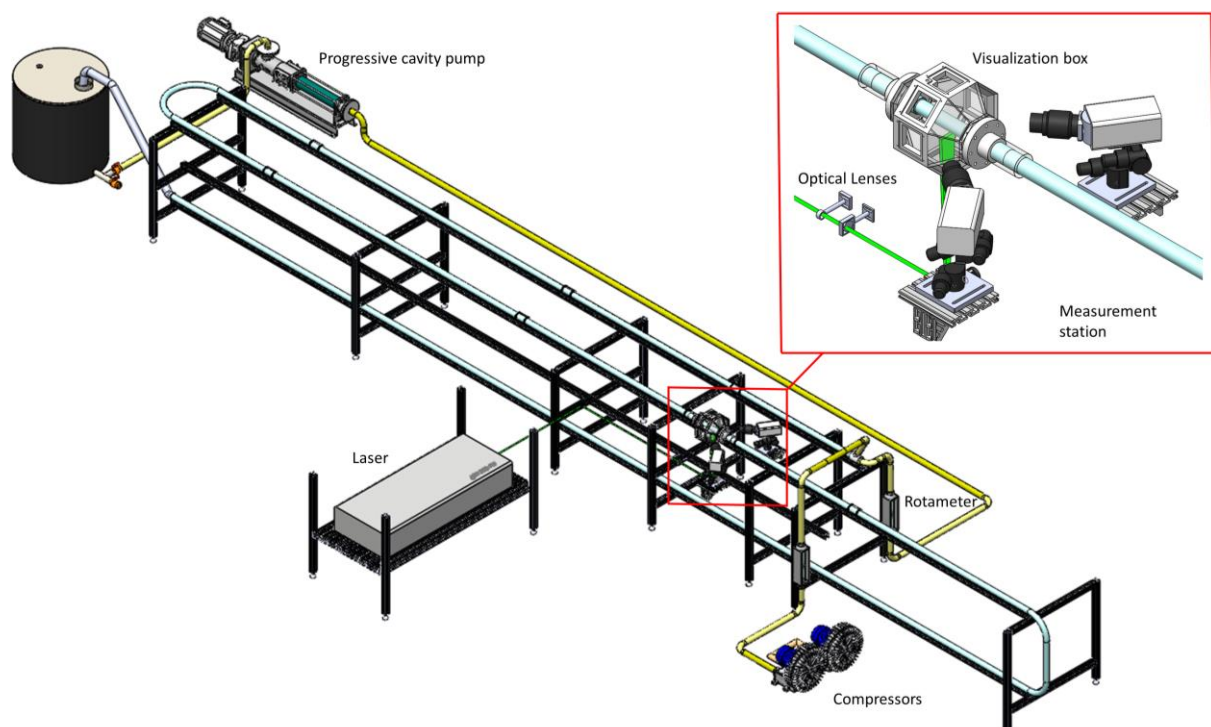


Figure 1 – Schematic view of the test section.

Fernandes et al. (2018) and allowed the determination of averaged velocity fields at know positions inside both the liquid plug and liquid film.

Measurements were performed with water superficial velocities of $J_L = 0.3, 0.4$ and 0.5 m/s and air superficial velocity of $J_G = 0.5$ m/s (cases 1, 2 and 3, respectively), corresponding to a mixture Reynolds numbers Re_m ranging from 32000 to 40000. Averaged velocity fields at different positions related to the gas-bubble nose were calculated based on 1500 unit cells passing through the measurement section.

3. RESULTS AND DISCUSSION

The averaged bubble translational velocity was calculated based on at least 400 instantaneous measurements, by the infrared photogate system. The increasing values obtained of $U_b = 1.11; 1.24$ and 1.32 m/s for $J_L = 0.3, 0.4$ and 0.5 m/s and $J_G = 0.5$ m/s constant are consistent with expressions found in the literature (Hurlburt and Hanratty, 2002).

A schematic with cases 1, 2 and 3 streamwise velocity profiles at 4 different positions, related to the gas-bubble nose tip, is presented in Fig. 2. It is clear the influence of the faster-moving gas-bubble on the velocity profiles at distances close to the gas-bubble nose tip (Fig. 2a and 2b), being this effect more evident to the case with higher mixture superficial velocity (case 3). As the distance to the gas-bubble increases, the averaged velocity field becomes independent of the distance to the gas-bubble nose (i.e., it develops). This effect is clear when comparing Fig. 2a and 2b to Fig. 2c and 2d.

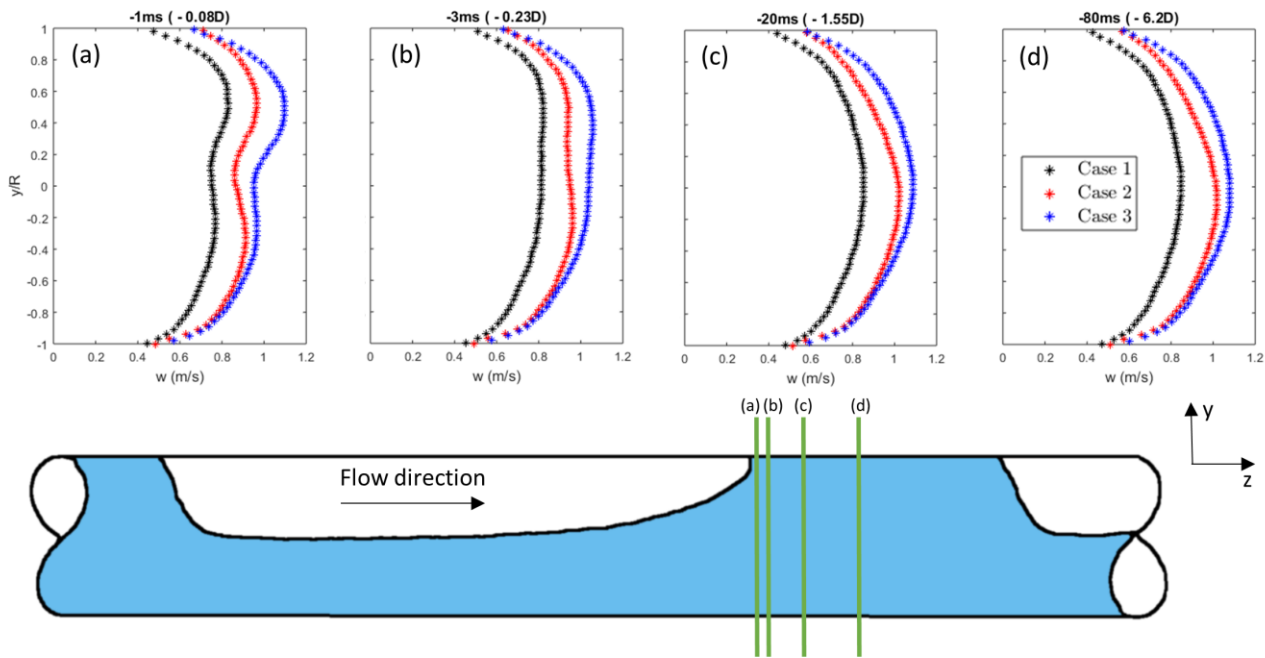


Figure 2 – Case 2 ($J_G = 0.5$ m/s and $J_L = 0.4$ m/s) streamwise velocity profiles at different positions related to the gas-bubble nose tip.

Since the gas and liquid superficial velocities are kept constant during the experiment, if one assumes an incompressible flow for both phases in the test section, continuity dictates that the total flow rate (and therefore, the mixture superficial velocity) are the same at any cross section within the slug unit cell (Woods and Hanratty, 1996). The average liquid velocity in the liquid plug should, therefore, be 0.8, 0.9 and 1.0 m/s for cases 1, 2 and 3. Table 1 shows a comparison of the expected value and the one obtained by averaging the measured velocity field at a position distanced of 6.2 D to the gas-bubble nose tip (Fig. 2d). An excellent agreement can be observed for cases 2 and 3, while a more considerable deviation was found in case 1.

Table 1 – Comparison of expected and measured averaged values in the liquid plug.

Case	Expected averaged liquid velocity	Measured averaged liquid velocity	Error
1	0.8 m/s	0.725 m/s	9.37%
2	0.9 m/s	0.905 m/s	0.55%
3	1.0 m/s	0.966 m/s	3.35 %

The small distance between each measurement plane, obtained by the high-frequency system employed, allowed the determination of the distance to the gas-bubble nose into which the velocity field in the liquid plug develops (i.e., it no longer varies in z coordinate). Figure 3 presents the root-mean-square deviation (RMSD between streamwise velocity vector fields, at different positions in the liquid plug and the one spaced $6.2 D$ to the gas-bubble nose tip (Fig. 2d). Calculations were performed through all cross sectional section of the pipe. Plotted values are normalized by the maximum RMSD, which happened at the closest position to the gas-bubble nose tip (Fig. 2a). It is clear that, for all cases, RMSD becomes almost constant around $0.8D$ from the gas-bubble nose tip, being this considered the development distance.

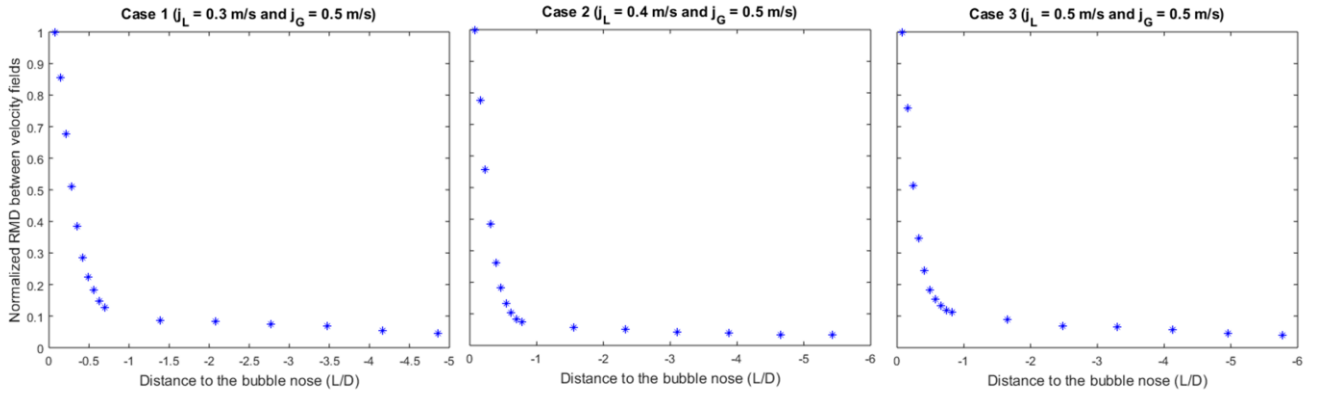


Figure 3 – Root-mean square deviation between averaged streamwise velocity fields at different positions in the liquid plug and the one spaced $6.2D$ to the gas-bubble nose tip for all three cases..

The friction velocity and, therefore, the wall shear stress were estimated based on the Clauser chart method (Clauser, 1956; Wei et al., 2005). This method assumes a universal logarithmic-law in the log-region, close to the wall pipe, as shown in Eq (1). U^+ and y^+ are the streamwise velocity and the wall-normal coordinate in inner scales, while k and C are the von Kármán empirical constants.

$$U^+ = \left(\frac{1}{k}\right) \ln(y^+) + C \quad (1)$$

Equation (1) can be re-written as Eq (2), where u_τ is the friction velocity and ν the kinematic viscosity. A small wall-normal possible error ε was added to consider the possibility of small deviations between the measured and real coordinates.

$$\frac{u}{u_\tau} = \left(\frac{1}{k}\right) \ln\left(\frac{y+\varepsilon}{\nu/u_\tau}\right) + C \quad (2)$$

The von Kármán empirical constants (B and k) were assumed as those suggested by George (2007). Equation 2 is then solved employing the least squares method, using the averaged velocity profiles, to find both u_τ and ε . Only velocity data at positions with y^+ greater than 50 and lower than 300 were used, as an attempt to guarantee that all points are within the log-layer. The wall shear stress τ_w is then calculated by Eq (3), where ρ is the fluid density.

$$u_\tau = \sqrt{\tau_w/\rho} \quad (3)$$

Figure 4 shows the result of the linear regression performed. Plots are in semi-log and in inner scales. A summary of the values which returned the lowest errors between the log law curve and the data are presented in Tab. 2.

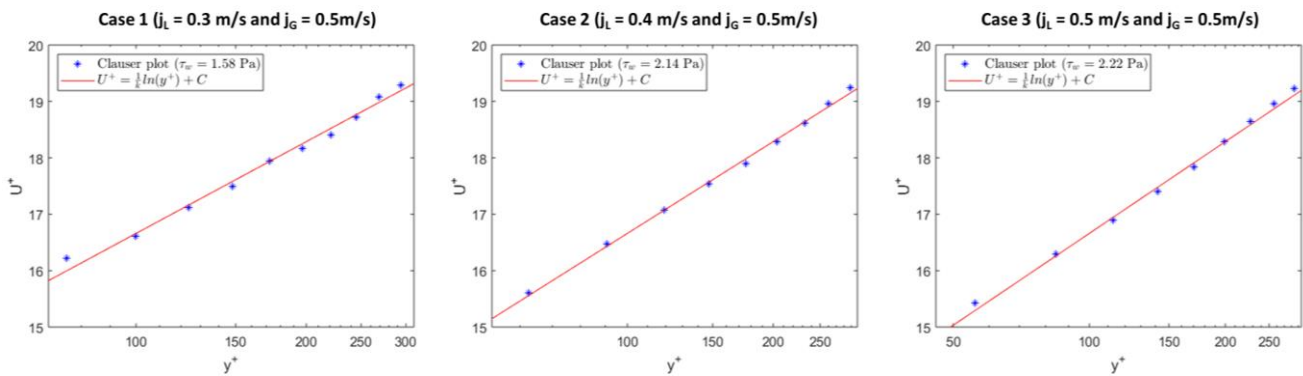


Figure 4 – Comparison between velocity data (blue marks) and theory (red line). Inner scales determined by the wall shear stress obtained by the Clauser method for all three cases.

Table 2 – Summary of the main parameters used in the Clauser Method and results obtained.

Case	ε (mm)	τ_w (Pa)	u_τ (m/s)	k	C
1	-1.64	1.58	0.0396	0.426	5.85
2	-0.48	2.14	0.0463	0.426	5.85
3	-0.4	2.22	0.0471	0.426	5.85

Given the fact that Fig. 3 shows that the variations in the velocity profiles within the liquid plug are small after a certain distance of the gas-bubble nose, the data presented here can be used to the development or validation of models to the wall shear stress in the liquid plug region.

4. CONCLUSION

The intermittent gas-liquid flow in a horizontal pipe was studied by a high-frequency stereoscopic PIV system. The measured ensemble-averaged velocity profiles clearly show the influence of the faster-moving gas-bubble on the liquid velocity fields. An analysis was done to estimate both the liquid plug developing distance, to the gas-bubble nose tip, as well as the wall shear stress in the liquid plug. The information presented is relevant both to the proper understating of the physics governing the phenomenon as well to the improvement of 1-dimensional numerical models.

5. ACKNOWLEDGEMENTS

The authors would like to acknowledge CAPES, CNPQ and Petrobras for the continuous financial support.

6. REFERENCES

- Al-Safran, E., Sarica, C., Zhang, H.Q. and Brill, J., 2005. Investigation of slug flow characteristics in the valley of a hilly-terrain pipeline. *International journal of multiphase flow*, 31(3), pp.337-357.
- Baker, O., 1953, January. Design of pipelines for the simultaneous flow of oil and gas. In Fall Meeting of the Petroleum Branch of AIME. Society of Petroleum Engineers.
- Brennen, C.E. and Brennen, C.E., 2005. Fundamentals of multiphase flow. Cambridge university press.
- Clauser, F.H., 1956. The turbulent boundary layer. In *Advances in applied mechanics* (Vol. 4, pp. 1-51). Elsevier.
- Fabre, J., Peresson, L.L., Corteville, J., Odello, R. and Bourgeois, T., 1990. Severe slugging in pipeline/riser systems. *SPE Production Engineering*, 5(03), pp.299-305.

- Fernandes, L.S., Martins, F.J. and Azevedo, L.F., 2018. A technique for measuring ensemble-averaged, three-component liquid velocity fields in two-phase, gas–liquid, intermittent pipe flows. *Experiments in Fluids*, 59(10), p.147.
- Hua, G., Falcone, G., Teodoriu, C. and Morrison, G., 2011, January. Comparison of multiphase pumping technologies for subsea and downhole applications. In *SPE Annual Technical Conference and Exhibition*. Society of Petroleum Engineers.
- Hurlburt, E.T. and Hanratty, T.J., 2002. Prediction of the transition from stratified to slug and plug flow for long pipes. *International journal of multiphase flow*, 28(5), pp.707-729.
- Ishii, M. and Hibiki, T., 2010. *Thermo-fluid dynamics of two-phase flow*. Springer Science & Business Media.
- Issa, R.I. and Kempf, M.H.W., 2003. Simulation of slug flow in horizontal and nearly horizontal pipes with the two-fluid model. *International journal of multiphase flow*, 29(1), pp.69-95.
- Kvernvold, O., Vindøy, V., Sønntvedt, T., Saasen, A. and Selmer-Olsen, S., 1984. Velocity distribution in horizontal slug flow. *International journal of multiphase flow*, 10(4), pp.441-457.
- Mandhane, J.M., Gregory, G.A. and Aziz, K., 1974. A flow pattern map for gas–liquid flow in horizontal pipes. *International Journal of Multiphase Flow*, 1(4), pp.537-553.
- Taitel, Y. and Dukler, A.E., 1976. A model for predicting flow regime transitions in horizontal and near horizontal gas-liquid flow. *AIChE journal*, 22(1), pp.47-55.
- Wei, T., Schmidt, R. and McMurtry, P., 2005. Comment on the Clauser chart method for determining the friction velocity. *Experiments in fluids*, 38(5), pp.695-699.
- Woods, B.D., Hanratty, T.J., 1999. Influence of Froude number on physical processes determining frequency of slugging in horizontal gas-liquid flows. *International Journal of Multiphase Flow*, 25, pp 1195-1223.
- George, W.K., 2007. Is there a universal log law for turbulent wall-bounded flows? *Philosophical Transactions of the Royal Society A: Mathematical, Physical and Engineering Sciences*, 365(1852), pp.789-806.

7. RESPONSIBILITY NOTICE

The authors are the only responsible for the printed material included in this paper.